INSTITUTE OF PHYSICS PUBLISHING JOURNAL OF PHYSICS: CONDENSED MATTER

J. Phys.: Condens. Matter **15** (2003) 2875–2897 PII: S0953-8984(03)53650-5

Thermoluminescence of zircon: a kinetic model

A A Turkin[1], H J van Es[2], D I Vainshtein[2] and H W den Hartog[2,3]

[1] National Science Centre, Kharkov Institute of Physics and Technology, 1 Akademicheskaya str, 61108 Kharkov, Ukraine
[2] Solid State Physics Laboratory, University of Groningen, 4 Nijenborgh, NL-9747 AG Groningen, The Netherlands

E-mail: anatole.turkin@kipt.kharkov.ua, a.turkin@phys.rug.nl, h.van.es@phys.rug.nl, d.vainshtein@phys.rug.nl and h.w.den.hartog@phys.rug.nl

Received 18 September 2002, in final form 13 February 2003
Published 22 April 2003
Online at stacks.iop.org/JPhysCM/15/2875

Abstract

The mineral zircon, $ZrSiO_4$, belongs to a class of promising materials for geochronometry by means of thermoluminescence (TL) dating. The development of a reliable and reproducible method for TL dating with zircon requires detailed knowledge of the processes taking place during exposure to ionizing radiation, long-term storage, annealing at moderate temperatures and heating at a constant rate (TL measurements). To understand these processes one needs a kinetic model of TL. This paper is devoted to the construction of such a model. The goal is to study the qualitative behaviour of the system and to determine the parameters and processes controlling TL phenomena of zircon. The model considers the following processes: (i) Filling of electron and hole traps at the excitation stage as a function of the dose rate and the dose for both (low dose rate) natural and (high dose rate) laboratory irradiation. (ii) Time dependence of TL fading in samples irradiated under laboratory conditions. (iii) Short time annealing at a given temperature. (iv) Heating of the irradiated sample to simulate TL experiments both after laboratory and natural irradiation.

The input parameters of the model, such as the types and concentrations of the TL centres and the energy distributions of the hole and electron traps, were obtained by analysing the experimental data on fading of the TL-emission spectra of samples from different geological locations. Electron paramagnetic resonance (EPR) data were used to establish the nature of the TL centres. Glow curves and 3D TL emission spectra are simulated and compared with the experimental data on time-dependent TL fading. The saturation and annealing behaviour of filled trap concentrations has been considered in the framework of the proposed kinetic model and compared with the EPR data associated with the rare-earth ions Tb^{3+} and Dy^{3+}, which play a crucial role as hole traps and recombination centres. In addition, the behaviour of some of the SiO_m^{n-} centres has been compared with simulation results.

[3] Author to whom any correspondence should be addressed.

1. Introduction

Ionizing radiation from natural radioactivity produces free charge carriers in non-conducting solids, which are partly trapped in the crystal lattice at crystal defects and/or impurities. Luminescence is caused by the stimulation of trapped electrons/holes from metastable energy levels (which are associated with defects and impurities), and their subsequent recombination at particular ions followed by light emission. The latent luminescence builds up with the passage of time, since trapped charge carriers accumulate with time. Controlled measurement of the intensity of the luminescence can be used for dosimetry or dating, i.e. for the determination of the time elapsed since the luminescence was last drained from the sample. The dating 'clock' resetting occurs each time the minerals in sand, silt or pottery are heated or exposed to sunlight. This dating technique is now widely used as a chronological tool in geological and archaeological studies.

Zircon, $ZrSiO_4$, belongs to a class of minerals, which exhibit luminescence after exposure to ionizing irradiation. Zircon is a very promising dating medium, because it is found around the world in many different types of sediment. Zircon has been widely studied because of several important applications including geochronology and immobilization of radioactive nuclear waste materials. In the early 1970s investigators established (see, for example, [1–7]) that zircon can be used for TL geochronometry. But later more attention was given to TL of quartz and optically stimulated luminescence (OSL) dating with quartz and feldspars [8–12] (see also [13] and references cited therein).

Most zircon crystals contain trace amounts of uranium and thorium, which irradiate the material internally at dose rates much higher than those from external sources. It is important for dating purposes that zircon is irradiated internally, whereas quartz is irradiated by external radiation sources, which depend both on time and on the detailed properties of the location, and hence cannot be reliably determined. During an internal alpha-decay event the energetic recoil atom produces a displacement cascade of about 1000 atoms and the alpha particle produces several hundred isolated atomic displacements. At high radiation doses zircon becomes heavily damaged, or even sometimes amorphous (metamict), as shown by diffraction experiments [14, 15]. The main obstacle to the development of a zircon TL dating methodology is that zircon grains are often inhomogeneous and zoned [16, 17], which affect their luminescence properties. Zircon grains in sediment deposits vary in colour from transparent and colourless to pink, blue, violet, very dark and black. The luminescence properties of the grains reveal enormous variations as well. Any effort to develop a reliable TL dating method for zircon has to be aimed on improving the homogeneity of the sample. Extracting zircon grains from the sediment is not sufficient. Special techniques have been developed to select homogeneous grains of high optical quality [18, 19].

There is another crucial problem. To develop a reliable dating method we need clear knowledge about the underlying physical processes taking place in zircon during the excitation stage, post-irradiation treatments and TL measurements. Experimentally, zircon displays a TL signal with a complicated spectral distribution, as well as a complex temperature dependence and fading behaviour. It is clear that to understand the peculiarities of zircon luminescence and to assess the feasibility of zircon for dating one needs a kinetic model of the processes taking place prior to and during the TL measurements. In a short communication [20] presented at the *11th International Conference on Radiation Effects in Insulators* we have proposed such a model and offered a set of rate equations in order to describe: (i) the kinetics of filling of electron and hole traps during the excitation stage, (ii) the behaviour of the trap system during long-term storage at ambient temperatures or annealing at moderate temperatures, and (iii) the TL stage of the dating methodology.

Turkin *et al* [20] contains only a brief summary of some tentative results related to the kinetic model of zircon TL. The purpose of this paper is to give a detailed description of the model, allowing the reader to reconstruct the logic behind the model and reproduce the results. In this paper, we will continue the investigation of the model and simulate real experiments. In the next section we will introduce and discuss the simulation model. We will describe how we have chosen the values of the parameters for the numerical calculations. Our simulation includes: the excitation stage during natural and/or laboratory irradiation, the redistribution of the charge carriers over the available traps (time-dependent fading) and the TL measurements. Glow curves and 3D TL emission spectra are simulated and compared with the experimental data for TL fading. The saturation and annealing behaviour of the concentrations of filled traps is considered in the framework of the proposed kinetic model and compared with the EPR data obtained for the natural zircon, which had been irradiated with a 0.5 MeV electron accelerator.

A comprehensive consideration of the scenarios associated with the dating methodology, based on the zircon TL, will be published elsewhere[4] [21].

2. The model

2.1. Assumptions of the model

The model is based on the well-known descriptions of thermoluminescence (TL) in materials (see for example [24–26]). The energy absorbed from the ionizing radiation (external or internal) creates free electrons and holes in the electronic system of the material, which participate in the following processes:

- *Trapping by luminescent centres (LCs).* An impurity ion of a particular type can form a bound state with a free charge carrier (electron or hole). When the charge carrier of the opposite sign arrives to this filled trap, it recombines with the previously trapped charge, which results in the emission of a photon (radiative recombination). The property required to emit photons depends on the type of the impurity ion.
- *Trapping by non-radiative centres.* Free charge carriers can form bound states not only with LCs, but also with other various ions/molecular ions, the nature of which is frequently unknown. When the charge carrier of the opposite sign arrives to that filled trap, it recombines with the previously trapped charge, but the released energy dissipates without emission of photons (hence, these centres are called non-radiative).
- *Mutual recombination.* Free charge carriers of opposite signs can recombine in the matrix without trapping by LC and non-radiative centres.
- *Recombination with defects of opposite charge at trapping centres (both radiative and non-radiative).*
- *Thermally activated eviction of electrons and holes from traps.* A trapped electron/hole forms a bound state with a trapping centre. The binding energy of this state determines the lifetime or the disintegration probability of the bound state. The disintegration probability increases with increasing temperature.
- *Redistribution of electrons and holes between traps and LC due to thermal excitation into conduction and valence bands.* Charge carriers, which are produced in the system due to thermally activated eviction from filled traps, can be retrapped by all other empty traps (i.e. both LCs and non-radiative centres).

[4] In a short communication [22] we have presented the results of a successful application of kinetic modelling to simulate the processes relevant for dating.

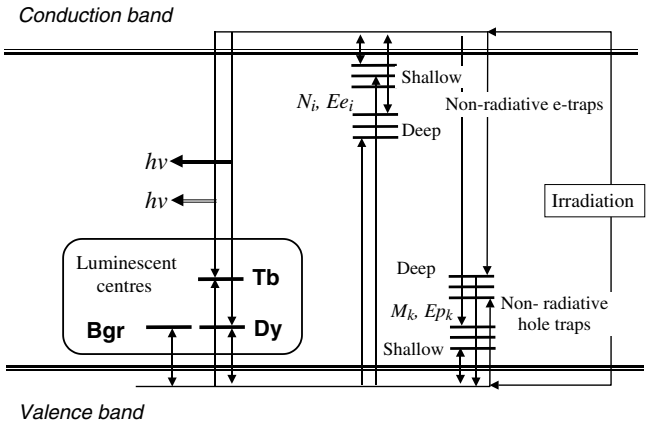

Figure 1. The band diagram representation of the electronic system of the mineral zircon. All allowed charge transitions are shown by arrows. Recombination events of electrons with holes trapped at Dy, Tb and background centres (Bgr) produce photons. N_i is the concentration of electron traps with energy Ee_i, $i = 1, \ldots, ie$. M_k is the concentration of hole traps with energy Ep_k, $k = 4, \ldots, kp$.

To keep in the model a minimum number of hypothesis it is assumed that electron and hole traps do not interact directly, i.e. there is no direct energy exchange between them. The traps are distributed randomly in the lattice without any spatial correlation. They interact only with free electrons and holes.

The terminology and possible transitions used in the model are shown in figure 1. The most important TL activators in zircon are Tb^{3+} and Dy^{3+} ions. The relation between the concentrations of Tb^{3+} and Dy^{3+} ions is similar for zircon from different locations and their values exceed the chondrite concentrations by two or three orders of magnitude [6]. This enhanced content of TL activator makes zircon an attractive mineral for dating. According to recent EPR investigations on natural zircon, Tb^{3+} and Dy^{3+} ions trap radiation-induced holes [23]

$$Tb^{3+} + \text{hole} \rightarrow Tb^{4+}, \qquad Dy^{3+} + \text{hole} \rightarrow Dy^{4+}. \tag{1}$$

We call Tb^{4+} and Dy^{4+} ions hole-type luminescence centres. In each recombination event of an electron with a hole trapped by LC there is a certain probability that a photon is emitted

$$Tb^{4+} + \text{electron} \rightarrow Tb^{3+} + \text{photon}, \qquad Dy^{4+} + \text{electron} \rightarrow Dy^{3+} + \text{photon}. \tag{2}$$

In addition to Tb^{3+} and Dy^{3+} centres, we have introduced into the model a third type of LC, which are called background centres. Experimentally at low temperatures, a rather broad distribution of emission wavelengths in the TL spectra is observed in the range 300–500 nm (figure 2(a)). We have found that the shape of this broad emission peak depends on the geological location from which the zircon samples were taken, while the position and shape of peaks due to Tb^{4+} and Dy^{4+} ions are well defined. We attribute the broad emission peak to some background LCs (Bgr centres). The nature of these centres is uncertain. Various impurities might be involved, the concentrations of which may depend on the history of the sample. The radiative recombination of the holes released from the shallow traps with electrons trapped at other centres and vice versa might contribute to this broadband TL-signal. For simplicity we include in the model only one type of Bgr LC and assume that below that the Bgr centres are

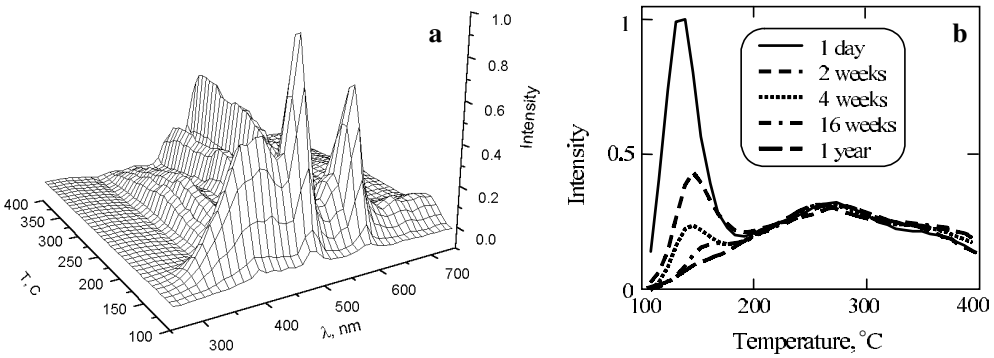

Figure 2. 3D TL emission spectra of a trail ridge sample after one day of fading (a) and glow curves for different fading times (b).

hole-type luminescence centres with a fixed trap depth. Their behaviour is similar to Tb and Dy ions.

$$\mathrm{Bgr}^{n+} + \mathrm{hole} \rightarrow \mathrm{Bgr}^{(n+1)+} \qquad \mathrm{Bgr}^{(n+1)+} + \mathrm{electron} \rightarrow \mathrm{Bgr}^{\mathrm{n}+} + \mathrm{photon}$$

where $n+$ denotes a hypothetical charge state of Bgr centres.

We have found that the above mentioned three hole-type radiative centres are sufficient to describe the fading experiments. The Tb^{3+} centres are assumed to be deep traps for holes, while the Dy^{3+} centres are shallow hole traps. The Bgr centres are shallow traps for holes, because the TL intensity associated with these centres and the TL signal from Dy^{4+} disappear at approximately the same temperature[5].

The remaining centres, denoted in figure 1 by N_i and M_k, are non-radiative. The non-radiative centres form two 'reservoirs', in which electrons and holes accumulate, depending on the trap type, by capturing these charge carriers during irradiation (excitation stage). During heating of the sample, luminescence occurs as a result of radiative recombination of electrons released thermally from occupied non-radiative centres with holes trapped at luminescence centres. The non-radiative electron traps have a rather wide and continuous distribution of binding energies (trap depth), otherwise one would observe narrow glow curves corresponding to electron traps with well defined binding energies instead of a broad tail-like feature (figure 2(b)). For symmetry reasons we take into account the effects of non-radiative hole traps distinct from radiative hole traps. As will be shown, shallow non-radiative trapping centres play a very significant role in the fading behaviour of TL from samples subjected to (high dose rate) laboratory irradiation.

2.2. Rate equations

The rate equations [20] describing the charge transfers shown schematically in figure 1 are similar to the rate equations of bimolecular chemical reactions. The concentrations of free electrons, which had been exited into the conduction band (n_c), free holes in the valence band (m_v), occupied non-radiative electron trapping centres (n_i) and occupied radiative and

[5] In principle, in a simplified version of the kinetic model the two emissions (due to Dy^{4+} and Bgr centres) can be connected with the existence of a single type of trap. However, we decided to include in the model Bgr centres. This makes the model more flexible, because it contains one more 'degree of freedom'.

non-radiative hole trapping centres (m_k) change with time in accordance with the following equations

$$\frac{\mathrm{d}n_c}{\mathrm{d}t} = K + \sum_i \nu_i^e(T) n_i - A_N n_c \sum_i (N_i - n_i) - A_m n_c \sum_k m_k - \alpha_e n_c m_v \tag{3}$$

$$\frac{\mathrm{d}m_v}{\mathrm{d}t} = K + \sum_k \nu_k^p(T) m_k - B_M m_v \sum_k (M_k - m_k) - B_n m_v \sum_i n_i - \alpha_e n_c m_v \tag{4}$$

$$\frac{\mathrm{d}n_i}{\mathrm{d}t} = A_N n_c (N_i - n_i) - B_n m_v n_i - \nu_i^e(T) n_i \tag{5}$$

$$\frac{\mathrm{d}m_k}{\mathrm{d}t} = B_M m_v (M_k - m_k) - A_m n_c m_k - \nu_k^p(T) m_k. \tag{6}$$

We do not write down the equations for the LCs separately, because the structure of the equations for hole traps is the same. Here, the subscript k refers to Tb ($k = 1$), Dy ($k = 2$), Bgr ($k = 3$) and non-radiative centres ($k = 4, \ldots, kp$).

Typically, during a TL experiment the sample temperature T is increased at a constant rate

$$\frac{\mathrm{d}T}{\mathrm{d}t} = \beta. \tag{7}$$

The nomenclature is similar to the one commonly used in the literature: n and m refer to electron and holes, respectively. All concentrations are dimensionless and defined per lattice site. In equations (3)–(7), N_i is the total concentration of electron traps with energy Ee_i, $i = 1, \ldots, ie$, $\nu_i^e = s_e \exp(-Ee_i/k_B T)$ is the electron detrapping rate, s_e is the frequency factor for trapped electrons, k_B is the Boltzmann constant, M_k is the total concentration of hole traps with energy Ep_k, $k = 1, \ldots, kp$ ($k = 1$, 2, 3 are reserved for Dy-, Tb- and Bgr-LCs, respectively), $\nu_k^p = s_p \exp(-Ep_k/k_B T)$ is the hole detrapping rate, s_p is the frequency factor for trapped holes, n_c is the concentration of free electrons, n_i is the concentration of traps occupied by electrons, m_v is the concentration of free holes, m_k is the concentration of traps occupied by holes, K is the production rate of electron–hole pairs per lattice site (ionization rate), and β is the heating rate during TL measurements.

The remaining parameters in the equations given above are the rate coefficients for trapping and recombination. The rate coefficients (transition probabilities) have the following meaning: α is the direct recombination of free electron and holes, A_N is the electron trapping by empty electron traps, A_m is the electron recombination with the hole trapped by hole traps, B_M is the hole trapping by empty p-traps, B_n is the hole recombination with the electron trapped by the electron non-radiative LC. For simplicity it is assumed that transition probabilities A and B do not depend on trap numbers i and k.

The physical meaning of the different terms in the set of equations can be explained conveniently by using the equation (3) for free electrons as an example

$\sum_i \nu_i^e(T) n_i$ thermally activated detrapping of electrons from all electron traps

$A_N n_c \sum_i (N_i - n_i)$ capture of free electrons by unoccupied electron traps

$A_m n_c \sum_k m_k$ annihilation of free electrons with trapped holes

$\alpha_e n_c m_v$ mutual recombination of free electrons with free holes.

The intensity of the luminescence is defined here as the rate with which photons appear per lattice site. When we ignore the internal optical absorption, the intensity is equal to the

recombination rate of electrons with holes trapped by LCs, i.e. a fraction of the energy released in one recombination event is transformed into a photon

$$I_{\mathrm{Tb}}(t) = A_m n_c m_{\mathrm{Tb}}, \qquad I_{\mathrm{Dy}}(t) = A_m n_c m_{\mathrm{Dy}}, \qquad I_{\mathrm{Bgr}}(t) = A_m n_c m_{\mathrm{Bgr}}. \tag{8}$$

In the case of a TL experiment with a constant heating rate, the intensity of the luminescence depends on the time or the temperature (equation (7)). The intensity of the luminescence can be analysed in terms of the luminescence spectra of the active species, if the probability $\Phi_i(\lambda)$ (i = Tb, Dy, Bgr) for LCs to emit light with wavelength λ is known

$$I(t, \lambda) = I_{\mathrm{Tb}}\Phi_{\mathrm{Tb}}(\lambda) + I_{\mathrm{Dy}}\Phi_{\mathrm{Dy}}(\lambda) + I_{\mathrm{Bgr}}\Phi_{\mathrm{Bgr}}(\lambda). \tag{9}$$

The integral intensity (total number of photons) emitted during the TL experiment as a function of irradiation dose ϕ is given by

$$I_{total}(\phi) = \int_0^{t_{TL}} I(t, \lambda, \phi)\,\mathrm{d}t\,\mathrm{d}\lambda = \int_0^{t_{TL}} G(t, \phi)\,\mathrm{d}t \tag{10}$$

where t_{TL} is the duration of the TL measurements, $I(t, \lambda, \phi)$ is the spectral distribution of the TL intensity (9) at a given dose ϕ, which is usually plotted in the form of a 3D TL picture. The glow curve is defined by the function

$$G(t, \phi) = \int I(t, \lambda, \phi)\,\mathrm{d}\lambda. \tag{11}$$

Because the time and the temperature during TL measurements are related by $T = T_0 + \beta t$, $G(t, \phi)$ is usually plotted as a function of temperature, the acquired dose being a fixed parameter.

The set of equations are well suited to consider the kinetics of charge transfer between traps during irradiation and heating. To describe the bleaching processes during exposure to light (optical bleaching) additional terms can be incorporated into the set of equations. It is therefore possible, in principle, to simulate OSL during exposure to light by the introduction of wavelength-dependent excitation probabilities.

In the next step we will specify the parameters used for our numerical simulations of the processes taking place during radiation-induced excitation, fading and the TL experiment.

3. Model parameters

The parameters presented in table 1 can be grouped into two categories: the fixed parameters that were not changed and fitting parameters, such as the concentrations and energies of TL centres and the energy distributions of the hole and electron traps.

The rate of production of free electrons and holes is defined per lattice site. This rate under natural conditions depends on the concentrations of radioactive impurities and their decay rates. In the present paper it is assumed that natural irradiation generates approximately one electron per second in zircon grains with a diameter of 120 μm, which corresponds to the ionization rate K_{Nat} (table 1). Here, it is also assumed that 2 days of laboratory irradiation corresponds to the natural dose acquired in about 9.4×10^4 years. The time of the laboratory irradiation indicated in the table 1 corresponds to a real irradiation using a ^{127}Cs γ-source, with a dose rate of 2.57 Gy min^{-1} and a total dose of 10 kGy [6].

The rate coefficients α, A_N, A_m, B_M and B_n for trapping and recombination are frequently defined as the product of the carrier thermal velocity and the interaction cross-section of the trapping centre (divided by atomic volume if concentrations are defined per lattice site). These

Table 1. Material parameters.

Mean atomic volume of zircon, ω (m^{-2})	1.05×10^{-29}
Electron trapping coefficient, α_e (s^{-1})	2×10^{17}
Hole trapping coefficient, α_p (s^{-1})	1×10^{17}
Rate coefficients for trapping and recombination	$A_N = A_m = \alpha_e$ $B_M = B_n = \alpha_p$
Electron attempt frequency for detrapping, s_e (s^{-1})	10^{14}
Hole attempt frequency for detrapping, s_p (s^{-1})	2.5×10^{13}
Rate of production of free electron and holes under natural conditions, K_{Nat} (s^{-1})	1.2×10^{-17}
Rate of production of free electron and holes under γ-irradiation (^{127}Cs γ-source, dose rate 2.57 Gy min^{-1}), K_{lab} (s^{-1})	2×10^{-10}
Rate of production of free electron and holes under e^- irradiation (electron linear accelerator, dose rate 15 kGy min^{-1}), K_{Acc} (s^{-1})	1.56×10^{-6}
Sample age, t_{Nat}, years	10^4
Time of laboratory γ-irradiation, t_{lab} (days)	2.7
Time of irradiation in electron linear accelerator, t_{Acc} (min)	15
Temperature of the sample during irradiation and fading, T_0 (°C)	20
Heating rate in TL experiment, β (°C s^{-1})	2.5
Heating rate from room temperature to annealing temperature, β_a (°C s^{-1})	2.0
Concentration of Tb, $M_1 = M_{\mathrm{Tb}}$ (ppm) (ppm $= 10^{-6}$)	40
Binding energy of a hole trapped at a Tb^{3+} ion, E_{Tb} (eV)	1.9
Concentration of Dy, $M_2 = M_{\mathrm{Dy}}$ (ppm)	80
Binding energy of a hole trapped at a Dy^{3+} ion, E_{Dy} (eV)	1.2
Concentration of background LC, $M_3 = M_{\mathrm{Bgr}}$ (ppm)	90
Binding energy of a hole trapped at a background LC, E_{Bgr} (eV)	1.2

coefficients can also be estimated as the rate of diffusion-controlled bimolecular reaction. According to [27], the reaction rate constant α_{ij} between species i and j is given by

$$\alpha_{ij} = \frac{4\pi r_{ij}}{\omega}(D_i + D_j) \tag{12}$$

where D_i and D_j are the diffusion coefficients, r_{ij} is the distance of closest approach between species i and j and ω is the mean volume per lattice site. Let us estimate, for example, the rate coefficient A_n

$$A_n = \frac{4\pi r_{trap}}{\omega} D_e = \frac{4\pi r_{trap}}{\omega} \frac{k_B T}{e} \mu_e \tag{13}$$

where r_{trap} is the trapping distance, e is the elementary charge. and μ_e is the electron mobility connected with the diffusion coefficient D_e by the Einstein relation. The typical order of magnitude of μ_e in crystalline semiconductors at room temperature is 10^{-2}–10^{-1} $m^2\ V^{-1}\ s^{-1}$ [28]. If we use for r_{trap} the mean radius of the atoms in zircon and the estimate for $\mu_e = 10^{-2}\ m^2\ V^{-1}\ s^{-1}$, we obtain from (13) $A_n = 4.2 \times 10^{16}\ s^{-1}$ at room temperature. For simplicity, similar to other models (developed, for example, for quartz [12]), the rate coefficients are assumed to be temperature independent. This can be justified by the fact that the major temperature effects come from thermally activated detrapping described by the factors $\nu^{e,p}$. As a first step in the development of the model the electron trapping coefficients are assumed to be the same for all traps (table 1). A more detailed description is not possible at present. The hole trapping coefficient is taken to be smaller than that for electrons because the mobility of the holes is usually smaller than the electron mobility. We checked the sensitivity of the model to changes in $\alpha_{e,p}$. It turned out that the simulation results (the shape of glow

and annealing curves, as well as fading behaviour) are insensitive to changes in $\alpha_{e,p}$ by several orders of magnitude, provided that $\alpha_{e,p}$ fulfill the conditions

$$\alpha_e \sum_i N_i \gg 1\ \mathrm{s}^{-1}, \qquad \alpha_p \sum_k M_k \gg 1\ \mathrm{s}^{-1}. \tag{14}$$

The physical reason is that under these conditions the trapping of free charge carriers occur very quickly (see equations (16) below), therefore the TL is controlled by the detrapping rates $\nu^{e,p}$. In other words, thermally activated detrapping acts as a bottleneck in the TL process.

3.1. Parameters of electron and hole traps

The concentrations of the TL centres and the energy distributions of the hole and electron traps were deduced from experimental data and the corresponding simulation results. The model parameters were varied systematically to obtain a good fit to the available experimental data.

For parameter selection the emission spectra of Trail Ridge (Florida, USA) samples were analysed, which had been exposed to γ-irradiation with high dose rate followed by fading at room temperature (i.e. storage in the dark) [6]. For samples with fading times of less than four weeks, at low temperatures (100–200 °C) the spectra are dominated by two narrow peaks due to Dy^{4+} superimposed on an unknown, unresolved emission band; at temperatures $T > 200$ °C only a six-line Tb^{3+} signal is present (figure 2). Since both Dy^{3+} and Tb^{3+} are hole traps and are expected to have similar TL properties, in order to explain the difference in their luminescent behaviour it is reasonable to assume that:

(i) the atomic concentration of Tb is less than the corresponding value for Dy, which is confirmed by measurements of the rare-earth element concentrations using laser ablation-inductively coupled plasma-mass spectroscopy [6],
(ii) the binding energy of holes with Dy^{3+} ions is smaller than that for Tb^{3+}, i.e. Dy^{3+} ions act as shallow traps for holes (table 1).

During TL Dy^{4+}, Tb^{4+} and $Bgr^{(n+1)+}$ centres simultaneously intercept detrapped electrons and give rise to simultaneous Dy^{3+}, Tb^{3+} and Bgr^{n+} emissions. However, the contributions of the different types of luminescence centre to the TL signal depend on the temperature. At low temperatures ($T < 200$ °C, figure 2) the Dy^{4+} centres are thermally stable, and their concentration is higher than the concentration of the Tb^{4+} centres, i.e. recombination of electrons with Dy^{4+} centres produces a TL signal that is stronger than the one from Tb^{4+} ions. Additionally, there is a broadband emission from Bgr centres. Because of the relatively small binding energy between Dy^{3+} ions and holes, at temperatures $T > 170$ °C the Dy^{4+} centres decompose thermally by releasing trapped holes, therefore after this they do not contribute to TL. With increasing temperature, the Bgr component of the TL signal disappears simultaneously with the TL signal associated with Dy^{4+}. For this reason we assume that the trapping energy of Bgr centres is close to that of Dy^{3+}. There is only one component that dominates the TL spectrum at elevated temperatures. This component is due to Tb^{4+} ions (figure 2), which are thermally stable and can be transformed into Tb^{3+} ions only by recombination with electrons released from non-radiative electron traps.

Another important experimental fact is that the well-defined low-temperature TL peak at $T < 200$ °C decreases during fading at room temperature and it ultimately disappears completely (figure 2(b)). This observation cannot be explained simply by the thermal eviction of holes from the active Dy^{4+} centres, otherwise after storage in the dark one would observe in this temperature range a high peak associated with recombination of electrons with Tb^{4+} ions. In order to account for the disappearance of low-temperature peaks in the glow curve during fading (figure 2(b)), we have to assume that after (high dose rate) laboratory irradiation there

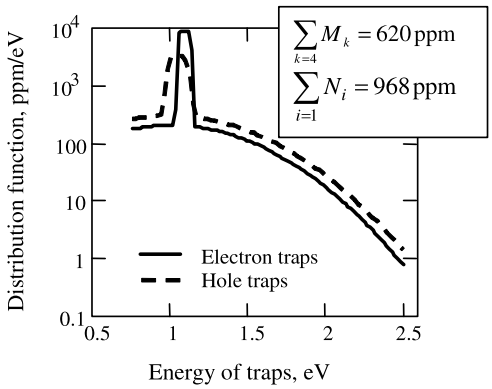

Figure 3. Distribution functions $f_e(Ee_i)$ and $f_p(Ep_k)$ of non-radiative electron and hole traps. The peak around 1 eV controls the fading behaviour, while the shape of the distribution functions at higher energies influence the shape of the Tb-emission for $T > 200\,^{\circ}$C.

are a lot of electrons in the system which have been trapped by shallow traps, and which can be released very easily during heating, giving rise to a high TL intensity at low temperatures (100–200 °C). Mathematically this implies that the energy distribution of the electron traps has a peak at about 1 eV below the bottom of the conduction band (figure 3). During storage in the dark the electrons, which are released from these traps, are detrapped at a very low rate; they look for deeper traps or recombine with holes, i.e. the amount of 'fuel' for low-temperature TL decreases with time, which is recorded as fading of the low-temperature TL. Since the fraction of occupied shallow traps is determined by the balance between the filling rate (ionizing irradiation) and thermal excitation rate, one should expect a very low occupancy of the shallow traps during natural irradiation; hence, no low-temperature TL peaks.

Even though the studied zircon samples were optically transparent (not heavily damaged or metamict), above 200 °C the emission from Tb^{3+} ions is continuous rather than peak-shaped (figure 2). Such a behaviour indicates that during TL the filled electron traps release electrons continuously. This implies that the energy distribution of the depths of the electron traps should be wide. Traps with a well defined trap depth release electrons in a certain temperature interval, giving rise to a narrow TL peak. The observed continuous emission from Tb^{3+} ions can be regarded as a superposition of individual TL peaks. The distribution functions of the depths of the electron and hole traps and their total numbers, which were used in the numerical simulation, are shown in figure 3. The shape of the distribution functions was taken in the form of the sum of two Gaussian distributions, which correspond to the populations of the shallow traps and the deep ones. These distributions were adjusted to reproduce the glow curves and the fading behaviour observed experimentally. It does not make sense to consider traps with trap depths less than 0.75 eV, since the time period required for thermal excitation of the electrons/holes from these traps, $1/\nu^{e,p}$, is less than 0.3 s at room temperature. Simulations have shown that the results are more sensitive to changes in the distribution function of electron traps than to changes in the distribution function of hole traps.

The emission spectra of the Tb, Dy and Bgr LCs were deduced using the experimental data on TL fading obtained for Trail Ridge (Florida, USA) samples and using the spectral distributions of the relevant TL components given by Iacconi and Caruba [29]. Figures 4(a) and (b) show the emission spectra for the sample after one day of fading. These spectra were approximated by analytical expressions (figures 4(c) and (d)) and then used in the calculations of 3D TL emission spectra. The low-temperature spectrum has been decomposed into a

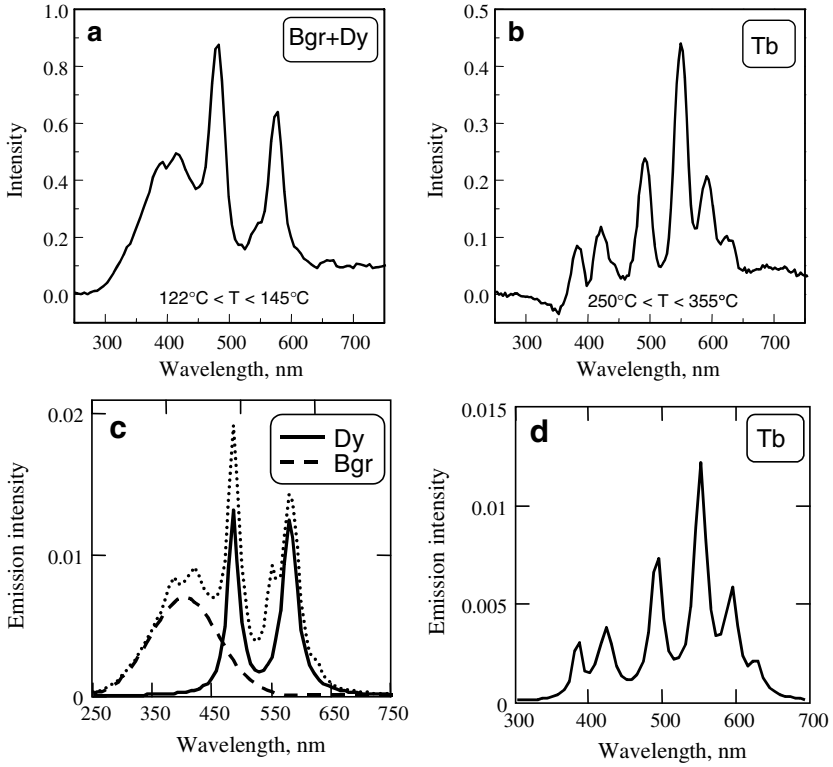

Figure 4. TL spectra of Dy, Bgr and Tb luminescence centres. (a), (b) Experimental TL spectra extracted from figure 2 and averaged over temperature intervals indicated in the figure. (c), (d) TL spectra used in our calculations. The dotted curve in (c) shows the sum of $\Phi_{\mathrm{Bgr}}(\lambda) + \Phi_{\mathrm{Dy}}(\lambda) + 0.5\Phi_{\mathrm{Tb}}(\lambda)$.

Dy spectrum and a Bgr contribution. The spectra shown in figures 4(c) and (d) are normalized to unity, i.e. they represent the corresponding probabilities $\Phi(\lambda)\,\mathrm{d}\lambda$ to emit photons with wavelengths in the interval λ, $\lambda + \mathrm{d}\lambda$.

4. Results of numerical simulations

4.1. Method

The energy distributions of the hole and electron traps, presented in figure 3, were replaced by groups of discrete energy levels. The number of traps within a group depends on the spacing between levels ΔEe, ΔEp and the distribution functions, the trap depths of the electron and the hole traps

$$N_i = f_e(Ee_i)\Delta Ee, \qquad M_k = f_p(Ep_k)\Delta Ep. \tag{15}$$

For the spacing between the levels we have used $\Delta Ee = 0.018$ eV and $\Delta Ep = 0.02$ eV. A small spacing between successive energy levels guarantees that glow peaks due to electrons coming from different traps to recombine with a hole trapped at a LC will overlap, producing smooth glow curves, just as observed experimentally. The total number of coupled equations solved simultaneously is 193.

Inspection of the kinetic equations shows that the timescales of the concentration variations differ enormously. The concentrations of the free charge carriers change very rapidly with time and they adjust quickly to the current concentrations of the traps. When the system is far from saturation ($N_i \gg n_i$ and $M_k \gg m_k$) the timescales of the variations of n_c and m_v are given by

$$\tau_e = \left(\alpha_e \sum_i N_i\right)^{-1} \approx 5 \times 10^{-15}\ \text{s}, \qquad \tau_p = \left(\alpha_p \sum_k M_k\right)^{-1} \approx 1 \times 10^{-14}\ \text{s}. \tag{16}$$

The timescales of the variations of the concentrations of the occupied traps, $1/\nu_i^e$ and $1/\nu_k^p$, depend on the trap energy and the temperature. Consequently, they change in a wide range, from small fractions of a second to many hundred years. Mathematically this means that our set of equations is stiff. Stiffness occurs in a problem when there are two or more very different scales of the independent variable on which the dependent variables are changing. The general problem of stiff equations is that we are required to follow the variation in the solution on the shortest timescale to maintain the stability of the integration, even though accuracy requirements allow a much larger stepsize. Several methods have been developed to treat such systems [31–33]. The method used in this paper to solve the initial value problem for our set of ordinary differential equations is an implicit Runge–Kutta method of the order of five with an adaptive stepsize [33]. In addition to an intrinsic error control of the algorithm, the accuracy of the calculations is controlled by checking the charge neutrality, which is defined as the relative error in the determination of the total charge of the system:

$$Q_{rel} = \left(\sum_i n_i + n_c - \sum_k m_k - m_v\right)\left(\sum_i n_i + n_c\right)^{-1}. \tag{17}$$

The total charge of the system must be equal to zero. Throughout all simulations presented below, the value of Q_{rel} was always several orders of magnitude smaller than the relative error tolerance of the algorithm, which was preset to 10^{-7}.

4.2. Natural irradiation with low dose rate

4.2.1. Kinetics of charge separation. In this section we will present the results of simulations of natural room-temperature irradiation experiments of a sample 'characterized' by the material parameters given in table 1.

Figure 5(a) shows the kinetics of the charge accumulation in non-radiative traps. It is seen that the shallow traps (with trap depths less than 1.3 eV) saturate very early. Their contribution to distribution functions is small (figure 5(b)). The time dependence of the concentrations of the active Tb^{4+} and Dy^{4+} centres is shown in figure 6. Because of the small trap depth, the population of the Dy^{4+} luminescence centres saturates after ten years of natural irradiation. Only a very small fraction, less than 10^{-5}, of all Dy^{3+} ions is occupied by holes. Since the trap energy for the Bgr LC is the same as for Dy^{3+} ions (table 1), the occupancy of the Bgr centres is the same as for Dy^{4+} centres. During natural irradiation the concentrations of the free electrons and holes are extremely small, less than 10^{-20} ppm, because free defects, generated by irradiation, are trapped very rapidly by the available electron and hole traps.

4.2.2. Simulation of TL experiments after natural irradiation (natural TL). Here we present the results of a simulated TL experiment with a sample prepared as described in the previous section. The sample was heated at a constant heating rate β from 20 to 500 °C. It was found that at temperatures below 100 °C all processes in the trap system are very slow. As expected, the concentrations of filled traps of both types decrease with time (or with temperature, since $T = T_0 + \beta t$), whereas the concentration of free carriers increases (figure 7). There is a small

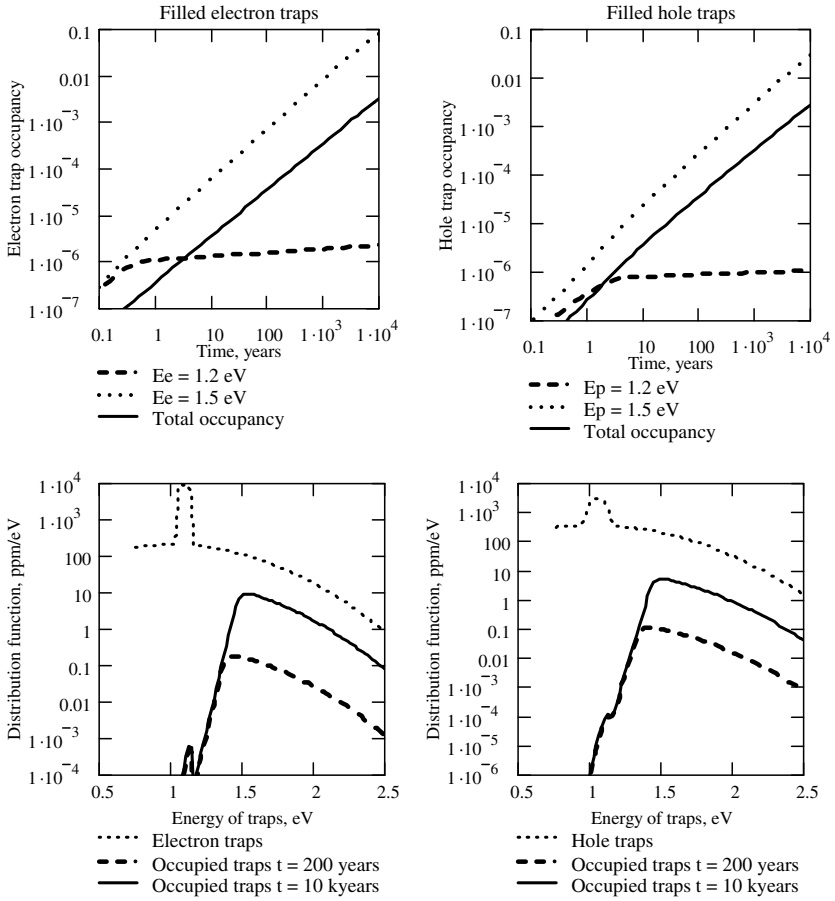

Figure 5. The kinetics of the charge accumulation in non-radiative traps in the case of natural irradiation. The upper panel shows the time dependence of the occupied fraction of non-radiative traps. The lower panel shows the distribution functions of the non-radiative electron (left) and hole (right) traps.

increase in the occupancy of Tb luminescence centres at about 300 °C due to a redistribution of the holes between traps with different trap depths.

Figure 8 shows the glow curves and the total TL intensity as a function of the age of the sample. Note the deviation from the linear behaviour for low doses in the plot showing the dose dependence of total intensity (figure 8(b)). According to figure 8(c) some traps may capture electrons, which are evicted thermally from other traps. However, the temporary increase in the occupancy of these traps does not influence the shape of glow curves. As will be seen in the next section, the redistribution of the electrons and holes over the available traps plays a more important role during fading and TL measurements after laboratory irradiation with high dose rates.

4.3. Laboratory irradiation

In order to compare the simulated results for laboratory irradiation with those obtained for natural irradiation, the same material parameters were used to simulate the laboratory

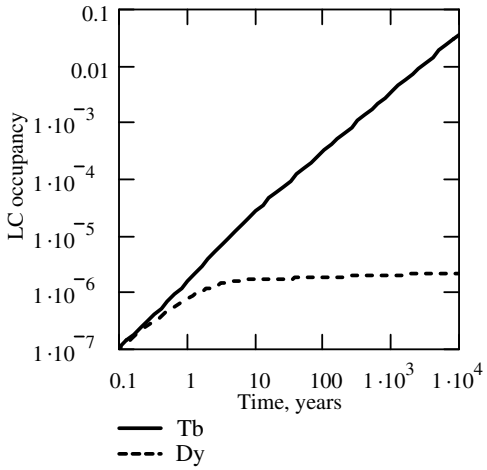

Figure 6. Fraction of Tb and Dy atoms with trapped electrons (active LC).

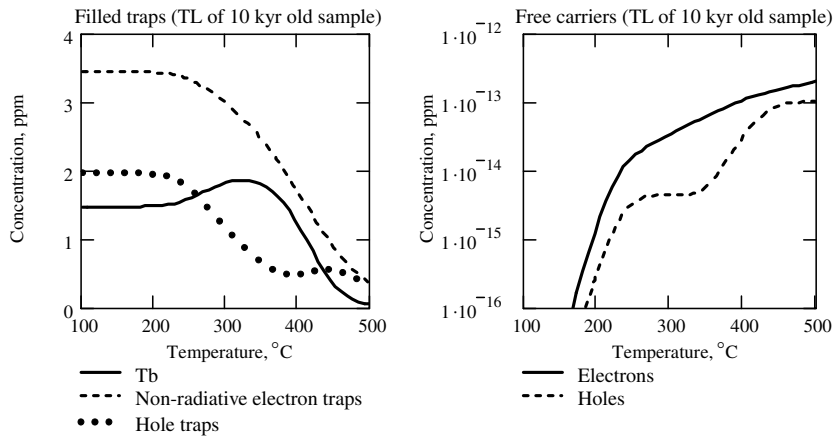

Figure 7. Dependence of the concentrations of the filled traps (left) and free charge carriers (right) on temperature during TL measurements.

irradiation for 2.7 days at room temperature. The dose rate of the laboratory irradiation is a factor of 10^7 higher than during natural irradiation (table 1). Therefore, as can be expected, the detailed balance in the trap system shifts towards higher occupancies of the shallow traps (compare the shape of distribution functions shown in figures 5(b) and 9). The distribution function for the occupied electron traps exhibits a peak, which will contribute to the luminescence between 100 and 200 °C during the simulated TL experiment. The model calculations have shown that the accumulation of the occupied traps is approximately linear with time, i.e. the system is far from saturation for the chosen set of parameters. The fractions of the Dy, Tb and Bgr centres, which are occupied by holes, are the same.

After the simulation of the laboratory irradiation the fading process was simulated during a period of 1000 days. A considerable redistribution of electrons and holes between the traps is observed (figure 10). It is seen that electrons and holes are released from shallow traps and captured by deeper traps. As a result the concentrations of the active LC change dramatically,

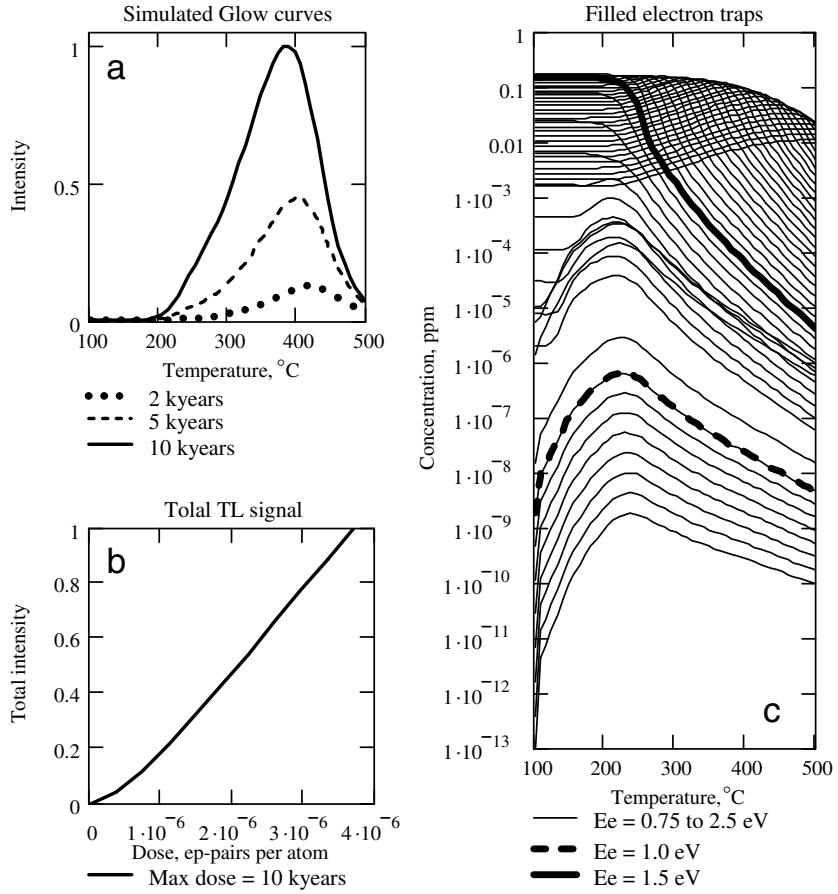

Figure 8. Simulation of a TL experiment after natural irradiation. (a) Glow curves of samples of different ages. (b) Total intensity of the TL signal as a function of irradiation dose (sample age). The maximum dose corresponds to 10^4 years. (c) Kinetics of the release of electrons from the population of non-radiative electron traps. Each curve represents the temperature dependence of the concentration of the filled traps with a fixed trap depth. The spacing between corresponding energy levels is 0.036 eV.

especially after prolonged fading (figure 10). The concentration of the Tb^{4+} centres increases at the expense of the holes released from shallow traps, while the Dy^{4+} centres decompose thermally.

5. Comparison of model predictions with experimental data

5.1. Simulation of TL experiments after fading

In this section the results of simulations of TL experiments after the laboratory irradiation and fading are presented. A considerable redistribution of electrons and holes over the available traps takes place, resulting in drastic changes in the concentrations of the active LCs. According to figure 11 the concentration of the Tb^{4+} centres increases at the expense of the shallow non-radiative traps, the Dy^{4+} and the Bgr centres.

A thermal generation of free electrons and holes is observed in the system during heating at temperatures higher than 100 °C (figure 12(a)). This leads to the appearance of a strong

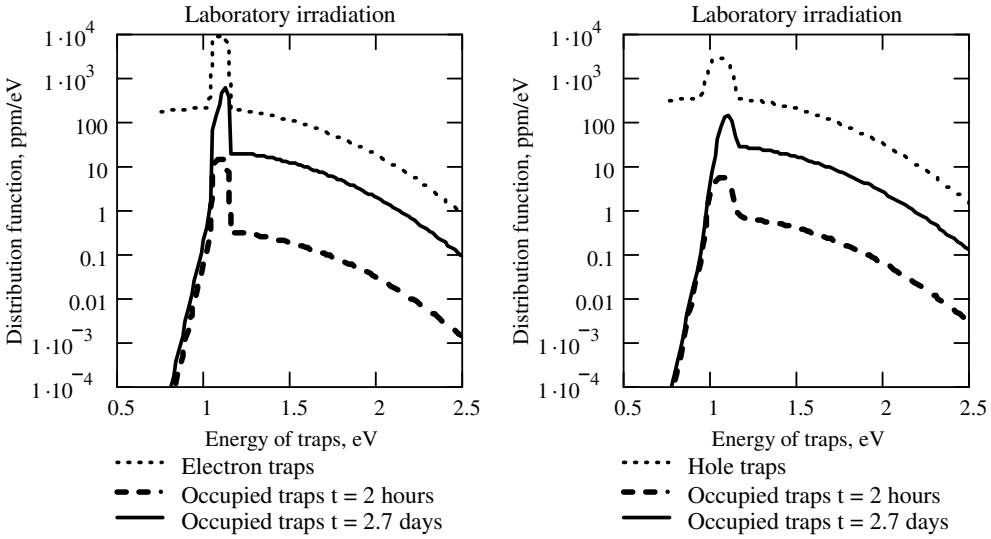

Figure 9. Distribution functions of non-radiative electron (left) and hole (right) traps, produced during laboratory irradiation.

luminescence peak (figure 12(b)), despite the decrease in the concentrations of the Dy^{4+} centres and Bgr LCs.

Let us compare the simulated results with real experimental data on TL fading of the Trail Ridge samples [6]. Figure 13(a) shows the simulated 3D emission spectra of the laboratory irradiated sample after one day of fading, which have been constructed using the emission probability functions $\Phi_i(\lambda)$ plotted in figure 4. The simulated glow curves are presented in figure 13(b). One can notice that figure 13 is very similar to figure 2 depicting experimental data. The time dependence of the fading of the TL signal is plotted in figure 14. It is seen that the simulated behaviour of zircon agrees quite well with the experimental data, especially in view of the uncertainty of the material parameters.

5.2. Kinetics of trapping centres in zircon after electron irradiation

The kinetic model described above has also been tested for various production rates of electrons and holes, and during annealing at several fixed temperatures. For the development of a reliable dating method we need information about the saturation behaviour of the trap concentrations as a function of the irradiation dose. A typical natural zircon crystal collects an internal radiation dose from the U and Th series elements of about 10 kGy during a time period longer than 10^4 years. Therefore, it is interesting to know at what dose saturation occurs. In [23] the EPR results on zircon, which had been irradiated to various doses with an electron accelerator, have been presented. Figure 15 shows the numerically calculated dose dependence of the Tb^{4+} concentration in zircon together with the intensity of the Tb^{4+} EPR lines. It is seen that the saturation of the Tb^{4+} concentration starts at a dose of about 100–150 kGy. The solid line represents the numerically calculated dose dependence of the Tb^{4+} concentration in zircon. The maximum number of filled Tb traps was found to be about 55–60% of the total number of available Tb impurities.

In [23] a series of the annealing experiments for some of the paramagnetic centres have been carried out at different temperatures. The model described above was used to explain the

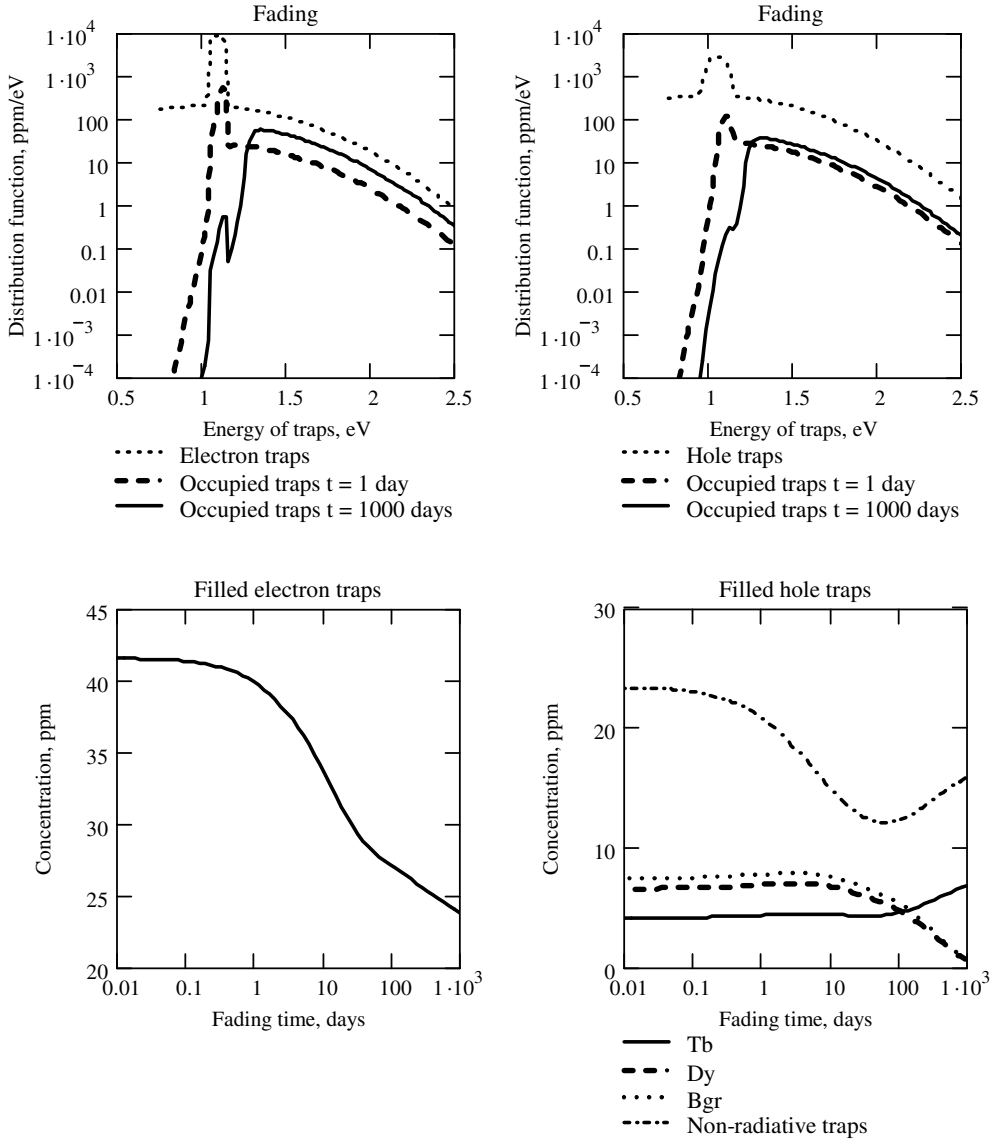

Figure 10. Redistribution of charge carriers over the traps during fading. The upper panel shows the distribution functions of non-radiative electron (left) and hole (right) traps, observed after laboratory irradiation followed by fading. Note the decrease in the fraction of occupied shallow traps. The lower panel shows the dependence of the filled trap concentrations on the fading time.

experimentally observed annealing behaviour of the SiO_2^{3-}, SiO_2^{3-} (II) centres and of the Dy^{4+} centre. The simulation of annealing experiment included the following steps:

(1) irradiation of the sample with a production rate of K_{Acc} (see table 1) for 15 min,
(2) fading for 3 h at room temperature to imitate the real situation when some time interval exists between the irradiation of the sample and the measurements,
(3) heating of the sample from room temperature to the annealing temperature at a rate β_a,
(4) annealing for 30 min at a fixed temperature.

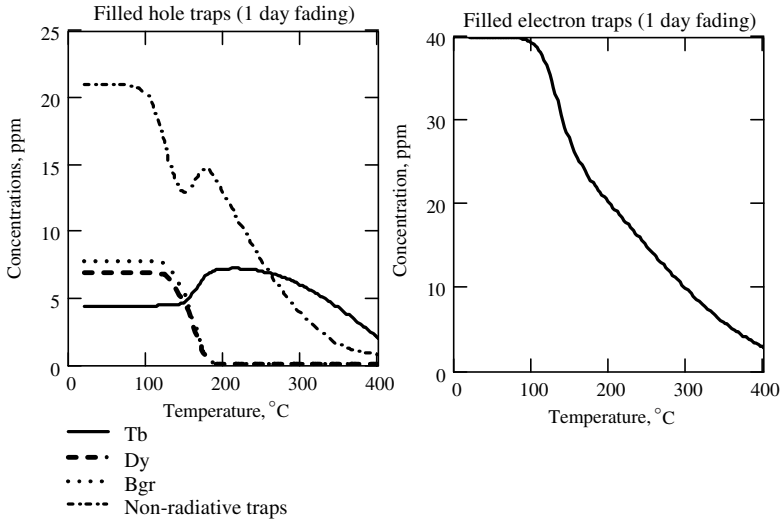

Figure 11. Dependence of the concentrations of filled electron traps (left) and filled hole traps (right) on temperature during the TL measurements after one day of fading.

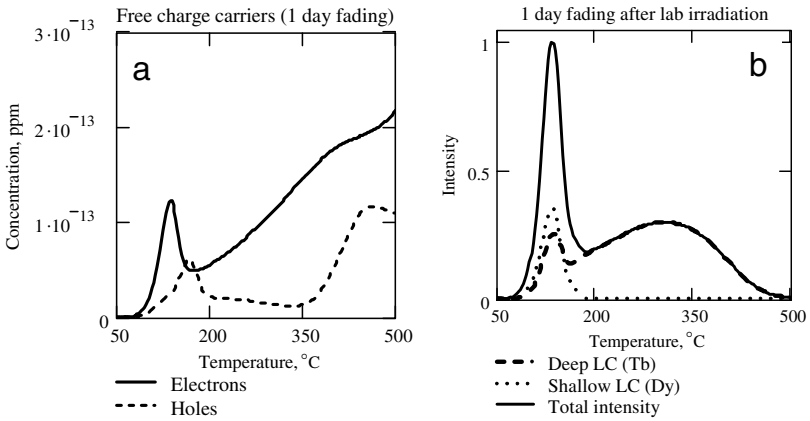

Figure 12. Thermal generation of free charge carriers (a) and the contribution of various LCs to the glow curve (b) for laboratory irradiated sample after one day of fading. The intensities are normalized to the maximum value of total intensity.

The SiO_2^{3-} centres were found to be the least stable ones of the paramagnetic class of radiation-induced defects [23]. In figure 16 we show the time dependence of the EPR intensity of the SiO_2^{3-} centres during annealing at 70 and 80 °C. The model calculations for the time dependence of the concentration of hole traps with $E_p = 1.12$ eV yield a good fit to the EPR data for the SiO_2^{3-} centres (figure 16).

The annealing behaviour of SiO_2^{3-} centres cannot be described by a simple exponential law, which is associated with one single, well-defined shallow trap. This means that different centres are involved in the annealing processes or different types of paramagnetic defect contribute to the EPR intensity in the temperature interval of the annealing experiment. As we have shown in previous sections, our interpretation is that the evolution of distributions of electron and hole

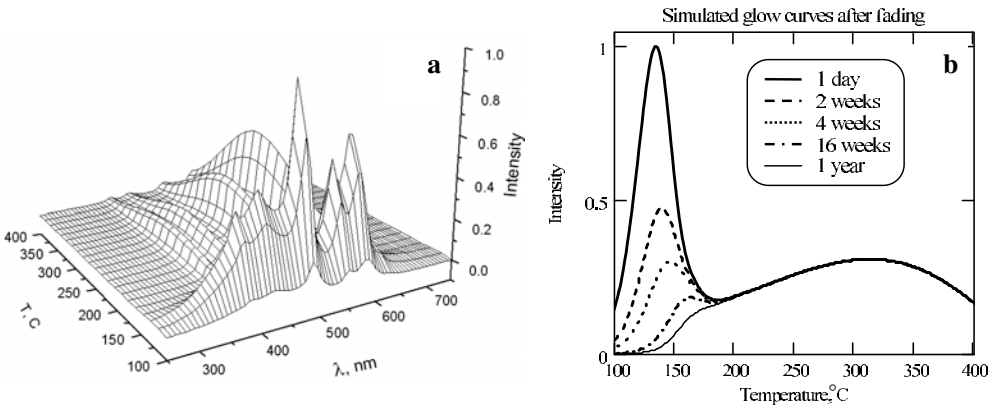

Figure 13. Simulated 3D TL spectra for the Trail Ridge (Florida, USA) samples [6] after laboratory irradiation followed by one day of fading (a) and glow curves for different fading times (b). The data were normalized to corresponding maximum intensities after one day of fading.

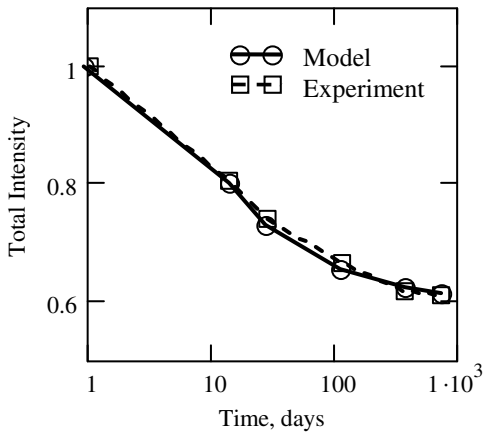

Figure 14. Decrease in the total TL signal as a function of storage time in darkness after laboratory irradiation. Comparison of the simulated results with the experimental data. The data were normalized to the maximum intensity after one day of fading.

traps is strongly coupled and the excitation of electron–hole pairs, trapping of free electrons and holes, redistribution of electrons and holes over the available traps, thermal excitation, subsequent retrapping and recombination processes, occur simultaneously.

The SiO_2^{3-}(II) centres are more stable than the SiO_2^{3-} centres [23]. Figure 17 depicts the dependence of the EPR intensity associated with the SiO_2^{3-}(II) centre versus the annealing time for different temperatures. The dependence is similar to that observed for the SiO_2^{3-} centre, however, it is quite clear that the SiO_2^{3-}(II) centre is more stable than the SiO_2^{3-} centre. The simulations show that an activation energy (i.e. a trap depth) of 1.52 eV can be associated with the hole-type SiO_2^{3-}(II) centre.

Figure 18 shows the results of a simulation of the annealing kinetics of Dy^{4+} luminescence centres ($E_{Dy} = 1.2$ eV, table 1) together with the corresponding intensities of the EPR signal observed for the Dy^{3+} centre. It is seen that the simulation results agree with the experimental data. Once more it should be emphasized that the annealing curves represent the

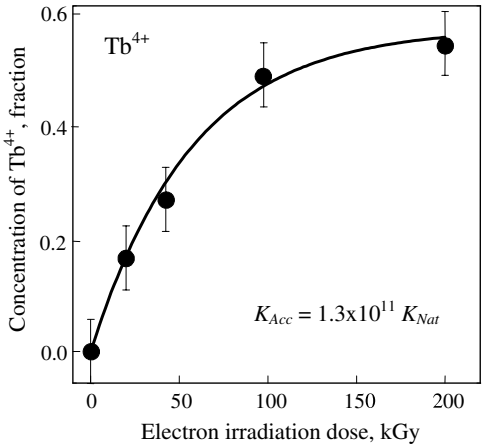

Figure 15. The fraction of Tb ions in zircon, which are occupied by holes (i.e. Tb^{4+}) as a function of the irradiation dose. The solid curve represents the dose dependence of the Tb^{4+} concentration calculated numerically with the kinetic model. The closed circles represent the experimental data, which are proportional to the intensity of the corresponding EPR lines. The irradiation of the crystals has been carried out with a linear electron accelerator.

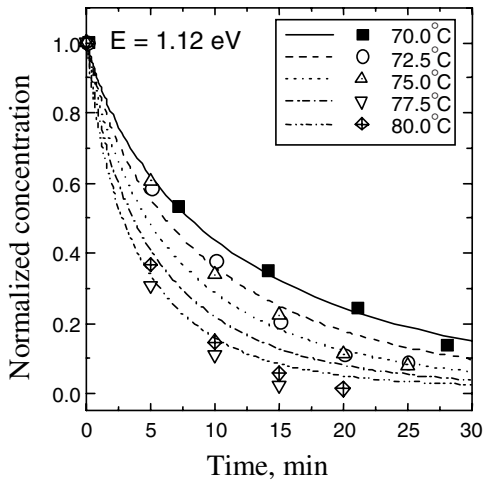

Figure 16. The dependence of the intensity of the SiO_2^{3-} EPR line, which is proportional to the concentration, versus the annealing time. The symbols show the experimental EPR intensity observed after annealing at different temperatures. The curves correspond to the simulated results for the concentration of the filled hole traps after annealing, using a fitted trap depth $E = 1.12$ eV.

behaviour of the trap system of zircon as a whole, rather than detrapping of holes from traps of single type. One can hardly expect to observe a simple exponential annealing behaviour for a system containing a broad distribution of trap depths. In fact the annealing curves represent the full history of the sample including excitation stage, fading and transient processes between different types of treatments. To illustrate this we present the time dependence of the concentration of different filled electron and hole traps (figure 19). Each curve corresponds to a trap with a fixed energy. It can be seen that some traps decompose thermally while the concentrations of other ones increase due to retrapping.

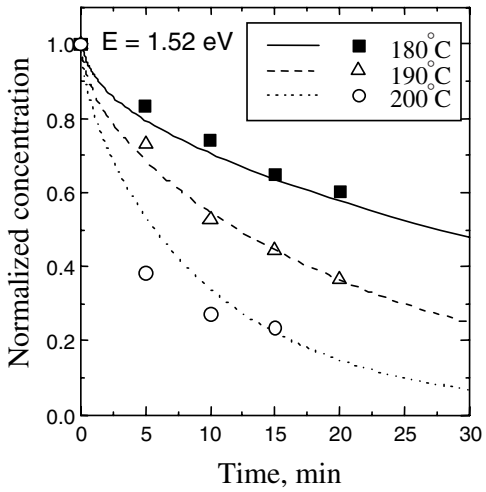

Figure 17. The dependence of the intensity of the SiO_2^{3-} (II) EPR line, which is proportional to the concentration, versus the annealing time. The symbols show the experimental EPR intensity. The curves correspond to the simulated results for the concentration of the filled hole traps using a trap depth $E = 1.52$ eV.

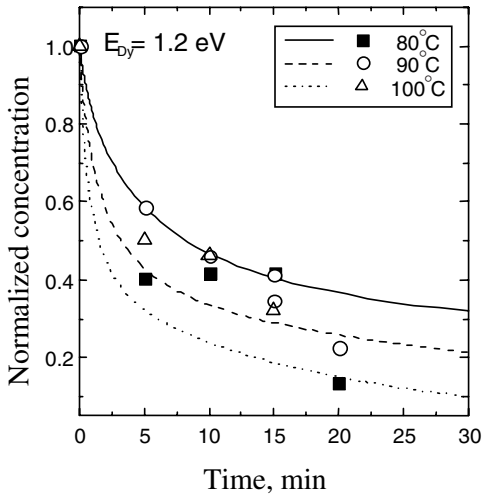

Figure 18. The dependence of the dysprosium concentration (the symbols indicate the intensity $I = I_{\max}^{EPR} - I^{EPR}$ of the Dy^{3+} EPR lines) versus the annealing time. The curves correspond to the simulated results for Dy^{4+} LCs, using a trap depth $E = 1.2$ eV.

It should be noted that the model parameters used here to explain the annealing results are the same as those used to describe TL fading. This is surprising and, at the same time, very encouraging. It demonstrates the potential advantages of these simulation studies, because with the model we are able to reproduce very different aspects of the behaviour of complex defect systems such as natural zircon. From a practical point of view this implies that the model might play an important role in the dating methodology for the TL medium zircon.

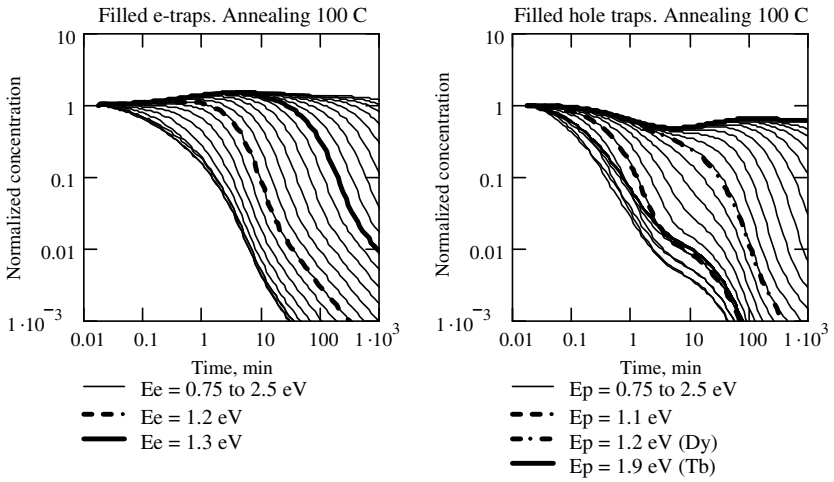

Figure 19. Simulation of the annealing process during 10^3 min. The sample was irradiated with dose rate K_{Acc} during 15 min. Each curve represents the concentration of the filled traps with a fixed trap depth. All concentrations are normalized to their initial values. The energy distances between successive trap levels are $\Delta Ee = 0.018$ eV and $\Delta Ep = 0.02$ eV, for electron and hole traps, respectively.

6. Conclusions

- A simulation model has been formulated to describe the processes related to TL of zircon including the excitation stage due to ionizing radiation, fading, annealing and TL measurements.
- A set of material parameters has been selected and adjusted to reproduce the experimental glow curves and the 3D TL emission spectra after laboratory irradiation followed by fading for up to two years. The same set has also been used successfully to describe the saturation and annealing behaviour of filled trap concentrations investigated by the EPR method.
- The model requires high concentrations of shallow electron and hole traps to explain the intense TL peaks due to Dy^{4+} after laboratory irradiation. Another important assumption of the model is that Dy^{3+} ions act as shallow traps for holes, whereas Tb^{3+} ions are deep hole traps.
- A significant redistribution of electrons and holes is observed in the trap system during storage in the dark after laboratory irradiation, as well as during annealing and during TL.
- Since the model proved to reproduce realistically very different aspects of the behaviour of a complex defect system such as natural zircon, the model can be used to design the optimum scenarios for TL dating with this mineral.

Acknowledgment

This research is supported by NWO-NATO grant no NB-67-34 and by the Technology Foundation STW (applied science division of NWO and the technology program of the Ministry of Economic Affairs) project GNS.4132.

References

[1] Wintle A G 1974 Factors determining the thermoluminescence of chronologically significant materials *PhD Thesis* Oxford University (unpublished)

[2] Sutton S R and Zimmerman D W 1976 Thermoluminescence dating using zircon grains from archaeological ceramics *Archaeometry* **18** 125–34

[3] Templer R H 1986 Auto-regenerative TL dating of zircon inclusions *Radiat. Prot. Dosim.* **17** 235–9
[4] Fain J, Miallier D, Montret M and Sanzelle S 1988 Zircon dating; regeneration and evaluation of the external dose *Nucl. Tracks Radiat. Meas.* **14** 333–7
[5] Smith B W 1988 Zircon from sediments; a combined OSL and TL auto regenerative dating technique *Quat. Sci. Rev.* **7** 401–6
[6] van Es H J, den Hartog H W, de Meijer R J, Venema L B, Donoghue J F and Rozendaal A 2000 Assessment of the suitability of zircons for thermoluminescence dating *Radiat. Meas.* **32** 819–23
[7] Huntley D J, Godfrey-Smith D I and Thewalt M L W 1985 Optical dating of sediments *Nature* **313** 105–7
[8] Wintle A G and Huntley D J 1982 Thermoluminescence dating of sediments *Quat. Sci. Rev.* **1** 31–53
[9] Roberts R, Walsh G L, Murray A, Olley R, Jones R, Morwood M J, Tuniz C, Lawson E, Macphail M, Bowdery D and Nauman I 1997 Luminescence dating of rock art and past environments using mud-wasp nests in northern Australia *Nature* **387** 696–9
[10] Olley J M, Caitcheon G C and Murray A S 1998 The distribution of apparent dose as determined by optically stimulated luminescence in small aliquots of fluvial quartz: implications for dating young sediments *Quat. Sci. Rev.* **17** 1033–40
[11] Murray A S and Wintle A G 2000 Luminescence dating of quartz using an improved single-aliquot regenerative-dose protocol *Radiat. Meas.* **32** 57–73
[12] Bailey R M 2001 Towards a general kinetic model for optically and thermally stimulated luminescence of quartz *Radiat. Meas.* **33** 17–45
[13] Bøtter-Jensen L 2000 Development of optically stimulated luminescence techniques using natural minerals and ceramics, and their application to retrospective dosimetry *Thesis Risø-R-1211(EN)* Risø National Laboratory Roskilde ISBN 87-550-2755-5 http://www.risoe.dk/rispubl/NUK/nukpdf/ris-r-1211.pdf
[14] Weber W J, Ewing R C and Wang L M 1994 The radiation-induced crystalline-to-amorphous transition in zircon *J. Mater. Res.* **9** 688
[15] Ríos S, Salje E K H, Zhang M and Ewing R C 2000 Amorphization in zircon: evidence for direct impact damage *J. Phys.: Condens. Matter* **12** 2401–12
[16] Nerurkar A P, De R, Chakraborty P N and Kaul I K 1979 Studies on thermoluminescence, metamictization and sintering properties of zircon sands *Mod. Geol.* **7** 13–24
[17] Templer R H and Walton A J 1985 Zoning in zircons *Nucl. Tracks* **10** 683–92
[18] van Es H J, Vainshtein D I, Rozendaal A, Donoghue J F, de Meijer R J and den Hartog H W 2002 Thermoluminescence of $ZrSiO_4$ (zircon): a new dating method? *Nucl. Instrum. Methods* B **191** 649–52
[19] van Es H J, den Hartog H W, Vainshtein D I, de Meijer R J, Donoghue J F and Rozendaal A 2002 Mineral zircon: a novel TL geochronometer? *(EURODIM 2002, Wroclaw, Poland); Rad. Eff. Defects Solids* **157** 1063–70
[20] Turkin A A, van Es H J, Vainshtein D I and den Hartog H W 2002 A kinetic model of zircon thermoluminescence *Nucl. Instrum. Methods* B **191** 37–43
[21] Turkin A A, van Es H J, Vainshtein D J and den Hartog H W 2003 Thermoluminescence of zircon: simulation of dating procedure, dose rate and temperature effects, at press
[22] Turkin A A, van Es H J, Vainshtein D J and den Hartog H W 2002 Protocol for TL dating with zircon: computer simulation of temperature and dose rate effects *(EURODIM 2002, Wroclaw, Poland); Rad. Eff. Defects Solids* **157** 833–38
[23] Laruhin M A, van Es H J, Bulka G R, Turkin A A, Vainshtein D J and den Hartog H W 2002 EPR study of radiation-induced defects in the TL dating medium zircon ($ZrSiO_4$) *J. Phys.: Condens. Matter* **14** 3813–31
[24] Horowitz Y S (ed) 1984 *Thermoluminescence and Thermoluminescent Dosimetry* vol 1–3 (Boca Raton, FL: Chemical Rubber Company Press)
[25] Aitken M J 1985 *Thermoluminescence Dating* (London: Academic)
[26] McKeever S W S and Chen R 1997 Luminescence Models *Radiat. Meas.* **27** 625–61
[27] Waite T R 1957 Theoretical treatment of the kinetics of diffusion-limited reactions *Phys. Rev.* **107** 463–70 2nd ser.
[28] Sze S M 1981 *Physics of Semiconductor Devices* 2nd edn (New York: Wiley)
[29] Iacconi P and Caruba R 1980 Trapping and emission centers in x-irradiated zircon. III. Influence of trivalent rare-earth impurities *Phys. Status Solidi* a **62** 589–96
[30] Press W H, Teukolsky S A, Vetterling W T and Flannery B P 1992 *Numerical Recipes in Fortran 77: The Art of Scientific Computing* 2nd edn (Cambridge: Cambridge University Press)
[31] Gear C W 1971 *Numerical Initial Value Problems in Ordinary Differential Equations* (Englewood Cliffs, NJ: Prentice-Hall)
[32] Kahaner D, Moler C and Nash S 1988 *Numerical Methods and Software* (Englewood Cliffs, NJ: Prentice-Hall)
[33] Hairer E and Wanner G 1996 *Solving Ordinary Differential Equations II. Stiff and Differential–Algebraic Problems (Springer Series in Comput. Math. vol 14, 2nd edn)* (Berlin: Springer)